academicJournals

Vol. 6(1), pp. 1-12, February 2014
DOI: 10.5897/JBSB2013.0045
ISSN 2141-2200 © 2014 Academic Journals
http://www.academicjournals.org/JBSB

Journal of Biophysics and Structural Biology

Full Length Research Paper

Spectroscopic approach of the interaction study of ceftriaxone and human serum albumin

Abu Teir M. M.[1*], Ghithan J.[1], Abu-Taha M. I.[1], Darwish S. M.[1] and Abu-hadid M. M[2].

[1]Department of Physics, Faculty of Science, Al-Quds University, Jerusalem, Palestine.
[2]Department of Immunology, Faculty of Medicine, Al-Quds University, Jerusalem, Palestine.

Accepted 18 November, 2013

Under physiological conditions, interaction between ceftriaxone and human serum albumin was investigated by using fluorescence spectroscopy and ultra violet (UV) absorption spectrum. From spectral analysis, ceftriaxone showed a strong ability to quench the intrinsic fluorescence of human serum albumin (HSA) through a static quenching procedure. The binding constant (k) is estimated as K=1.02× 10^3 M^{-1} at 298 K. Fourier transform infrared spectroscopy (FT-IR) spectroscopy with Fourier self-deconvolution technique was used to determine the protein secondary structure and drug binding mechanisms. The observed spectral changes indicated the formation of H-bonding between ceftriaxone and HSA molecules at higher percentage for α-helix than for the β-sheets.

Key words: Ceftriaxone, amide I-III, binding mode, binding constant, protein secondary structure, Fourier transform IR, UV-spectroscopy, Flurosence spectroscopy.

INTRODUCTION

In recent years, many investigations on the binding of drugs and natural products to human serum albumin (HSA) were carried out (Il'ichev et al., 2002; Qing et al., 2011; Ahmad et al., 2006; Liu et al., 2009). Ceftriaxone, as a possible ligand, was not studied in details upon its binding reaction with HSA. It has been reported that Ceftriaxone binds to HSA (Guowen et al., 2011, Bibiana et al., 1996).

Ceftriaxone, a cephalosporin, is bound reversibly to defatted human serum albumin from adults, with a first stoichiometric binding constant of $6x10^4$ M^{-1}, as found by equilibrium dialysis at pH 7.4, 37°C (Roberton et al., 1989). So far, none of the investigations determine in details the Ceftriaxone-HSA binding constant and the effects of Ceftriaxone complexation on the protein.

Ceftriaxone belongs to a group of antibiotics called the cephalosporins. It is a parenteral cephalosporin that displays a broad spectrum of activity against Gram-negative and Gram-positive pathogens; its chemical structure is shown in Figure 1 (Bilirubin et al., 1989). Ceftriaxone is indicated for a wide variety of infections. These include infections of the lower respiratory and urinary tracts, bacterial septicemia, skin and skin structure infections, bone and joint infections, pelvic inflammatory disease, uncomplicated gonorrhea, intra-abdominal infections, acute bacterial otitis media, meningitis, as well as surgical prophylaxis (Quaglia et al., 1997).

The drug is widely used because of its broad spectrum of antibacterial activity, infrequent side-effects, and long serum half-life and it has recently been recommended as the drug of choice for use in newborn infants exposed to Neisseria gonorrhea during delivery (Bibiana et al., 1996).

It has been reported that ceftriaxone is transported through the blood-brain barrier (Scott et al., 2008; Reynold et al., 1987) and it is widely accepted that some conformational diseases, such as Alzheimer's and prion diseases can be the result of misfolding due to lack of stability in parallel β-sheets (Locht et al., 1990). Recent reports suggest that somedrugs may accelerate these

*Corresponding author. E-mail: abuteir@science.alquds.edu.

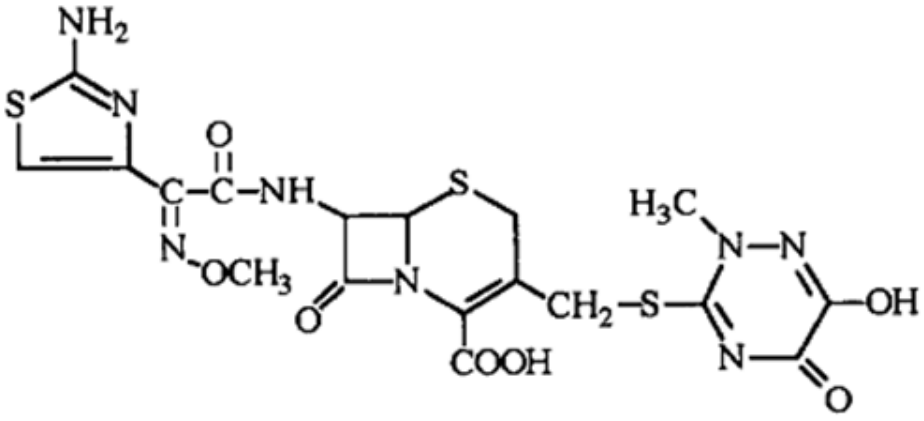

Figure 1. Chemical structure of ceftriaxone.

neurodegenerative diseases (Rabia et al., 2009). This emphasizes the needs to understand protein folding and sheets stability in some proteins complexes with drugs.

The widespread use of ceftriaxone and its transport through the blood-brain barrier makes it necessary to study structural changes of ceftriaxone -protein complexes to understand the biological effects and functions of ceftriaxone in the body. Thus, the study of ceftriaxone - protein interaction is of great interest in the field of biophysics, life sciences and clinical medicine.

HSA is the most abundant protein in human plasma, which is synthesized in the liver (Fengling et al., 2006) and is able to bind and thereby transport various compounds such as fatty acids, hormones, bilirubin, tryptophan, steroids, metal ions, therapeutic agents and a large number of drugs. HSA serves as the major soluble protein constituent of the circularity system, it contributes to colloid osmotic blood pressure, it can bind and carry drugs which are mainly poorly soluble in water (Peters et al., 1985). HSA accounts for approximately 60% of the total plasma protein corresponding to a concentration of 40 mg/ml in the blood (~0.6 mM) (Peters et al., 1985). The three dimensional structure of HSA was determined through x-ray crystallographic measurements (He et al., 1992). This globular protein consists of a single polypeptide chain of 585 amino acids (Hal et al., 2000), which have a molecular weight of 66 kDa (Bian et al., 2004). HSA composed of three homologous domains I, II and III, each containing two sub-domains, A and B, each having six and four α-helices, respectively (Curry et al., 1999). The tertiary structure of HSA is stabilized by 17 disulphide bridges giving it a heart shaped molecule (He et al., 1992; Bian et al., 2004).

It has been shown that distribution, free concentration, and metabolism of various drugs can be significantly altered as a result of their binding to HSA (Artali et.al, 2005; Kang et al., 2004). The binding properties of albumin depend on the three dimensional structure of the binding sites, which are distributed all over the molecule. Strong binding can decrease the concentrations of free drugs in plasma, whereas weak binding can lead to a short lifetime or poor distribution or both. Its remarkable capacity to bind a variety of drugs results in its prevailing role in drug pharmacokinetics and pharmacodynamics (Kandagal et.al, 2007).

Multiple drug binding sites have been reported for HSA by several groups of researchers (Bhattacharyya et al, 2006; Simard et al., 2006; Ulrich .et al., 2006). The principal regions of ligand binding sites of HSA are located in hydrophobic cavities in sub domains IIA and IIIA, which corresponds to site I and site II, respectively. Site I is dominated by strong hydrophobic interaction with most neutral, bulky, heterocyclic compounds, while site II mainly by dipole-dipole, van der Waals, and/or hydrogen-bonding interactions with many aromatic carbo-xylic acids. HSA contained a single tryptophan residue (Trp-214) in domain IIA and its intrinsic fluorescence is sensitive to the ligands bound nearby (Krishnakumar et al., 2002; Muravchick et al., 1995). Therefore, it is often used as a probe to investigate the binding properties of drugs with HSA.

The interaction of ceftriaxone sodium (CS), a cephalosporin antibiotic, with the major transport protein, bovine serum albumin (BSA), was investigated using different spectroscopic techniques such as fluorescence, circular dichroism (CD), and UV-vis spectroscopy (Cao et al., 2012). The mechanism of the interaction between bovine serum albumin (BSA) and ceftriaxone with and without zinc (II) (Zn^{2+}) was studied employing fluorescence, ultraviolet (UV) absorption, circular dichroism (CD), and synchronous fluorescence spectral methods. The intrinsic fluorescence of BSA was quenched by ceftriaxone in a static quenching mode, which was authenticated by Stern-Volmer calculations.

The binding constant, the number of binding sites, and the thermodynamic parameters were obtained, which indicated a spontaneous and hydrophobic interaction between BSA and ceftriaxone regardless of Zn^{2+} (Liu et al.,

2012).

In this study, we have investigated the interaction of ceftriaxone with HSA by means of FT-IR, UV/VIS, and fluorescence spectrophotometer. Infrared spectroscopy provides measurements of molecular vibrations due to the specific absorption of infrared radiation by chemical bonds. It is known that the form and frequency of the Amide I band, which is assigned to the C=O stretch-ing vibration within the peptide bonds is very characteristic for the structure of the studied protein.

From the band secondary structure, components peaks (α-helix, β-strand) can be derived and the analysis of this single band allows elucidation of conformational changes with high sensitivity (Abu et al., 2011). This work will be limited to the mid-range infrared, which covers the frequency range from 4000 to 400 cm^{-1}. This wavelength region includes bands that arise from three conformational sensitive vibrations within the peptide backbone (Amides I, II and III) of these vibrations. Amide I is the most widely used and can provide information on secondary structure composition and structural stability (Cui et al., 2008; Kang et al., 2004; Rondeau et al., 2007).

One of the advantages of infrared spectroscopy is that it can be used with proteins that are either in solution or in thin film. In addition there is a growing body of literature on the use of infrared to follow reaction kinetics and ligand binding in proteins, as will as a number of infrared studies on protein dynamics.

The identification of the binding sites in albumin was also performed using probes for the so-called sites I, II, bilirubin and fatty acids binding sites. Albumin showed two types of binding sites for cefoperazone and ceftria-xone, while for cefsulodin it showed a single type of bind-ing site (Pico et al., 1996).

The mechanism of the interaction between human serum albumin (HSA) and ceftriaxone has been studied by using UV, fluorescence and FTIR spectroscopy. Further-more temperature dependent conformation of HSA struc-ture at different concentrations of Ceftriaxone has been studied by FT-IR spectroscopy.

MATERIALS AND METHODS

Human serum albumin (HSA, 96-99% purity) and Ceftriaxone disodium salt hemi(heptahydrate) in powder form were pur-chased from Sigma Aldrich chemical company and used without further purification.

Preparation of stock solutions

HSA was dissolved in phosphate buffer saline, at physiological pH 7.4 at (80 mg/ml) concentration. Ceftriaxone with molecular weight of 66.5 kDa was dissolved in phosphate buffer saline (1.21 mg/ml), the solution was placed in ultrasonic water path (SIBATA AU-3T) for 6 h to ensure that all the amount of Ceftriaxone was completely dissolved. The final concentrations of HSA- Ceftriaxone complexes were prepared by mixing equal volume of HSA and Ceftriaxone stock solution. HSA concentration in all samples were fixed at 40 mg/ml (~0.6 mM). However, the concentration of Ceftriaxone in the final protein drug solutions was decreased gradually to attain the desired drug concentrations of 0.687, 0.910, 1.14, 1.37, 1.60, 1.83 and 2.06 mM. The solution of Ceftriaxone and HSA were incubated for 1 h (at 25°C) before spectro-scopic measurements were taken.

Fluorescence

The fluorescence measurements were performed by a Nano-Drop ND-3300 Fluorospectrometer at 25°C. The excitation had been done at the wavelength of 360 nm and the maximum emission wavelength was at 439 nm. The excitation source comes from one of three solid-state light emitting diodes (LED's). The excitation source options include: UV LED with maximum excitation of 365 nm, Blue LED with excitation of 470 nm, and white LED from 500 to 650 nm excitation. A 2048-element CCD array detector covering 400-750 nm, was connected by an optical fiber to the optical measurement surface. The emission spectra were recorded for free HSA 40 mg/ml (~0.6 mM) and for its complexes with ceftriaxone solutions with the concentrations of (0.687, 0.910, 1.14, 1.37, 1.60, 1.83, 2.06 mM). Repeated measurements were done for all samples and no significant differences were observed.

FT-IR spectroscopy experimental procedures

The FT-IR measurements were obtained on a Bruker IFS 66/S spectrophotometer equipped with a liquid nitrogen-cooled MCT detector and a KBr beam splitter. The spectrometer was conti-nuously purged with dry air during the measurements. The absorption spectra were obtained in the wave number range of 400-4000 cm^{-1}. A spectrum was taken as an average of 60 scans to increase the signal to noise ratio, and the spectral resolution was at 4 cm^{-1}. The aperture used in this study was 8 mm, since we found that this aperture gives best signal to noise ratio. Baseline correction, normalization and peak areas calculations were per-formed for all the spectra by OPUS software. The peak positions were determined using the second derivative of the spectra. The infrared spectra of HSA, and Ceftriaxone-HSA complex were obtained in the region of 1000-1800 cm−1. The FT-IR spectrum of free HSA was acquired by subtracting the absorption spectrum of the buffer solution from the spectrum of the protein solution. For the net interaction effect, the difference spectra [(protein and Ceftriaxone solution) - (protein solution)] were generated using the featureless region of the protein solution 1800-2200 cm^{-1} as an internal standard (Surewicz et al., 1993). The accuracy of this subtraction method is tested using several control samples with the same protein or drug concentrations, which resulted into a flat base line formation. The obtained spectral differences were used here, to investigate the nature of the drug-HSA interaction. We had also used ELAB 12/05 thermo system to directly and simultaneously determine the thermo-dependent structural changes of drug-protein complexes.

RESULTS AND DISCUSSION

Analysis of fluorescence quenching of HSA by Ceftriaxone

Fluorescence spectroscopy is one of the most widely used spectroscopic techniques in the fields of bioche-mistry and molecular biophysics today (Royer et al.,

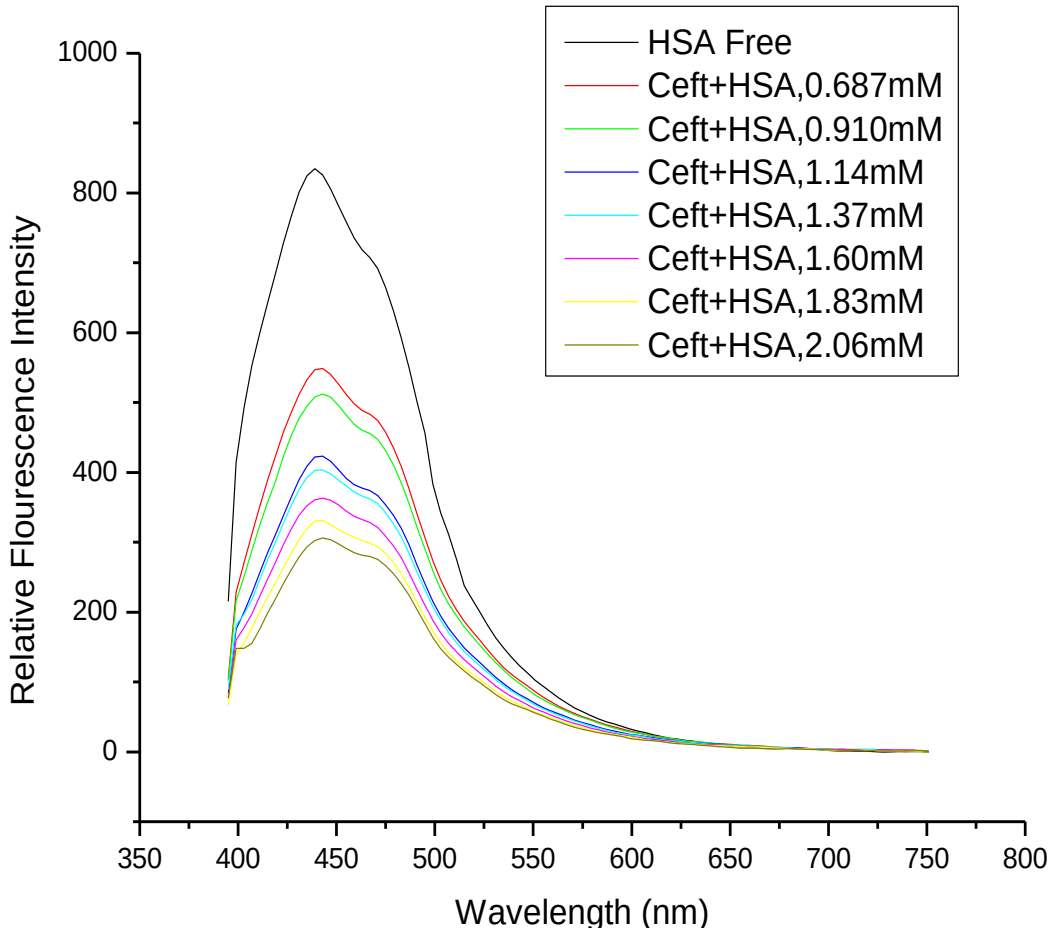

Figure 2. Fluorescence emission spectra of HSA in the absence and presence of ceftriaxone at different concentrations.

1995). Fluorescence measurements can give some information on the binding mechanism of small molecule substances to protein, including binding mode, binding constants, binding sites and intermolecular distances (Liu et al., 2004). The fluorescence of HSA comes from tryptophan, tyrosine and phenylalanine residues. Actually, the intrinsic fluorescence of HSA is almost contributed by tryptophan alone (Sulkowska et al., 2002).

Figure 2 shows the fluorescence spectra of HSA in the presence of various concentrations of ceftriaxone. It is obvious that HSA fluorescence intensity gradually decreased with the increase of Ceftriaxone concentration, while the peak position shows little or no change upon increasing the concentration of Ceftriaxone to HSA, indicating that Ceftriaxone binds to HSA. Under the same condition, no fluorescence of Ceftriaxone was observed hich indicates that Ceftriaxone could quench the auto fluorescence of HSA which confirm that Ceftriaxone interacts with HSA, leading to a change in the microenvironment around the tryptophan residue exposing it to the polar solvent (Wang et al., 2007; Cui et al., 2007).

Two mechanisms, namely dynamic quenching and static quenching are responsible for the fluorescence quenching. The possible quenching mechanism can be deduced from the Stern-Volmer plot. The dynamic quenching process can be described by the Stern-Volmer equation (Tian et al., 2003)

$$\frac{F_0}{F} = 1 + K_q \tau_0 [Q] = 1 + K_{sv} [Q] \quad (1)$$

Where, F_0 and F are the fluorescence intensities of HSA in the absence and presence of the quencher, respectively. Kq is the quenching rate constant of the biomolecule, K_{SV} is the Stern-Volmer dynamic quenching constant, and $K_{SV}=K_q\tau_0$. τ_0 is the average lifetime of the biomolecule without quencher. The value of τ_0 of the biopolymer was $10^{-8}s^{-1}$ (Chen et al., 1990), and [Q] is the concentration of quencher ceftriaxone.

The Stern-Volmer quenching constant Ksv indicates the sensitivity of the fluorophore to a quencher. Linear curves were plotted according to the Stern-Volmer

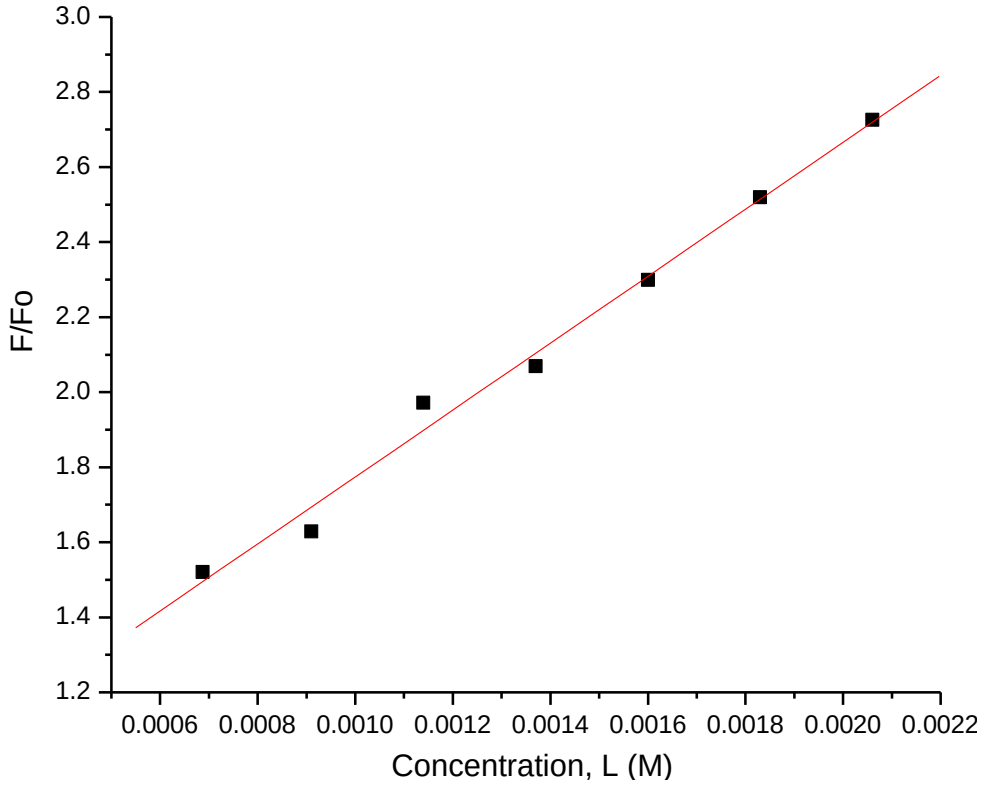

Figure 3. The Stern-Volmer plot for Ceftriaxone-HSA complexes.

equation as shown in Figure 3 for ceftriaxone- HSA complexes. The Stern-Volmer quenching constant Ksv was obtained by the slope of the curve obtained in Figure 3, and its value equals 8.92×10^{2} L mol^{-1}.

From the equation above, the value of $Ksv=Kq\tau_0$, can be used to calculate the value of Kq using the fluorescence life time of 10^{-8} s for HSA, to obtain Kq value of (8.92×10^{10} L $mol^{-1}s^{-1}$) for ceftriaxone- HSA complexes. Generally, the maximum dynamic quenching constant, Kq of various kinds of quenchers with biopolymer was 2.0×10^{10} L $mol^{-1}s^{-1}$ (Lakowicz et al., 1973).

Obviously, the values of kq were greater than that of the maximum dynamic quenching constant. This suggested that the fluorescence quenching was not the result of dynamic quenching, but the consequence of static quenching (Chen et al., 1990, Wang et al., 2008).

When static quenching is dominant, the modified Stern-Volmer equation could be used (Lakowicz, et al.1999).

$$\frac{1}{F_0 - F} = \frac{1}{F_0 KL} + \frac{1}{F_0} \quad (2)$$

Where, K is the binding constant of ceftriaxone with HSA, and can be calculated by plotting 1/(F0-F) vs. 1/L (Figure 4). The value of K was obtained from the values of slope and intercept, respectively. K equals the ratio of the intercept to the slope.

The value of K was 1.02×10^{3} M^{-1} at room temperature, which is consistent with the value obtained by Bibiana et al., (1996) and Patrick et al. (1990). *In vitro* protein binding studies were conducted to examine the interaction between ceftriaxone (CEF), probenecid (PROB) and diazepam (DIAZ). The presence of PROB and DIAZ at concentrations equal to molar albumin concentration caused a decrease in CEF affinity from 3.7 x 10^{4} M^{-1} (control) to 1.1 x 10^{4} (PROB) and 2.6 x 10^{4} (DIAZ) M^{-1}, but not in binding capacity in pooled human plasma (Stoeckel et al., 1990).

The value obtained is indicative of a weak Ceftriaxone-HSA interaction with respect to the other drug-HSA complexes with binding constants in the range of 10^{5} and 10^{6} M^{-1} (Kragh-Hansen et al., 1981). The highly effective quenching constant in this case has lead to a lower value of binding constant between the drug and HSA due to an effective hydrogen bonding between ceftriaxone and HSA.

FT-IR spectroscopy

FT-IR spectroscopy is a powerful technique for the study of hydrogen bonding (Li et al., 2006), and has been identified as one of the few techniques that is established

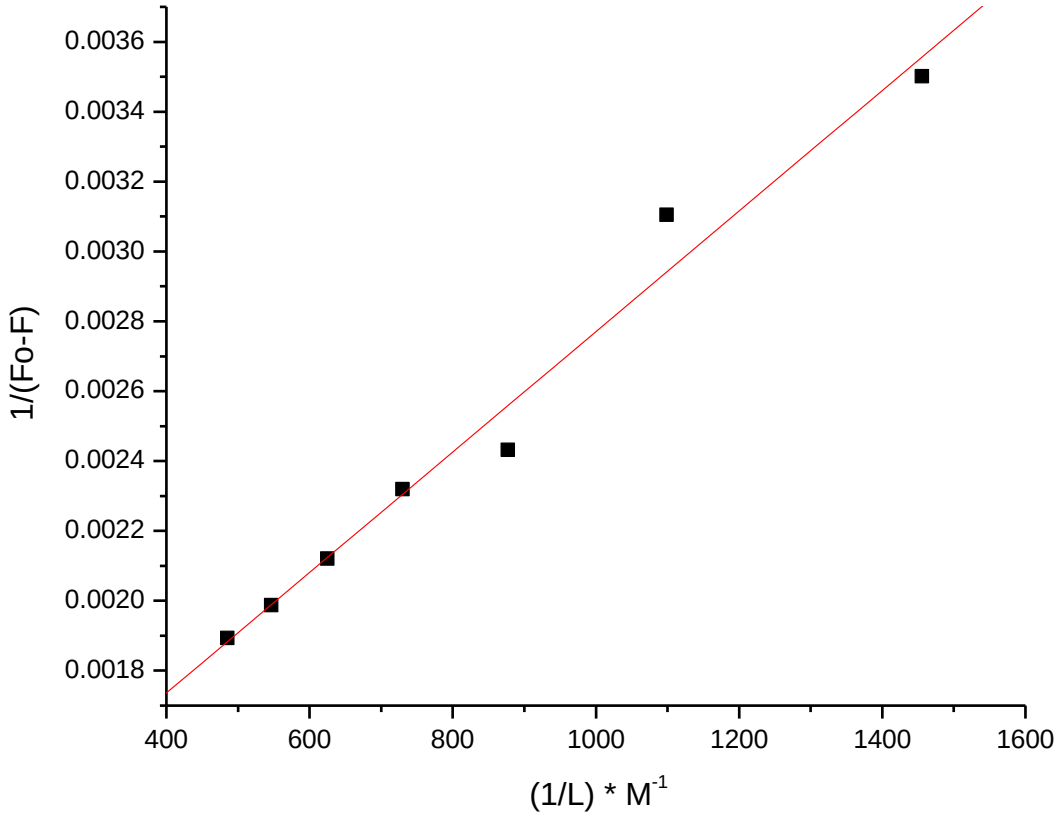

Figure 4. The plot of 1/(Fo-F) vs (1/L) for ceftriaxone- HSA complexes.

in the determination of protein secondary structure at different physiological systems (Sirotkin et al., 2001; Arrondo et al., 1993). The information on the secondary structure of proteins could be deduced from the infrared spectra. Proteins exhibit a number of amide bands, which represent different vibrations of the peptide moiety. The amide group of proteins and polypeptides presents characteristic vibrational modes (amide modes) that are sensitive to the protein conformation and largely been constrained to group frequency interpretations (Ganim et al., 2006).

The modes most widely used in protein structural studies are amide I, amide II and amide III. Amide I band ranging from 1700 to 1600 cm^{-1} and arises principally from the C=O stretching (Vandenbussche G et al., 1992), has been widely accepted to be used (Workman et al., 1998). The amide II band is primarily N-H bending with a contribution from C-N stretching vibrations; amide II ranging from 1600 to 1480 cm^{-1} while amide III band ranging from 1330 to 1220 cm^{-1} which is due to the C-N stretching mode coupled to the in-plane N - H bending mode (Arrondo et al., 1993; Jackson et al., 1991).

The second derivative of free HSA is shown in Figure 5A, where the spectra is dominated by absorbance bands of amide I and amide II at peak positions 1656 and 154 4cm^{-1}, respectively. Figure 5B, shows the spectrum of ceftriaxone- HSA complexes with different concentrations of ceftriaxone.

The peak positions of amide I bands in HSA infrared spectrum shifted as listed in Table 1: 1637-1642 cm^{-1}, 1655-1658 cm^{-1}, 1683-1679 cm^{-1}, 1693-1692 cm^{-1} after interaction with ceftriaxone. In addition, peaks at 1613 and 1626 cm^{-1} had disappeared and also a new peak at 1663 cm-1 had appeared after the interaction of ceftriaxone with HSA. In amide II, the peak positions have shifted as follows: 1496 to 1494 cm^{-1}, 1512 to 1513 cm^{-1}, 1544 to 1536 cm^{-1} and 1580 to 1584 cm^{-1}. In addition, a new peaks at 1552 and 1568 cm^{-1} appeared after the interaction of ceftriaxone with HSA. In the Amide III region little or no change of the peak positions has been observed. The changes of these peak positions and peak shapes implied that the secondary structures of HSA had been changed by the interaction of ceftriaxone with HSA. The minor changes in peak positions can be attributed to the effect of the newly formal H-bonding between ceftriaxone molecules with the protein. It is suggested that, the shift to a higher frequency for the major peak in amide I region (1656-1658 cm^{-1}) came as a result of stabilization by hydrogen bonding by having the C-N bond assuming partial double bond character due to a low of electrons from the C=O to the C-N bond (Jackson et al., 1991).

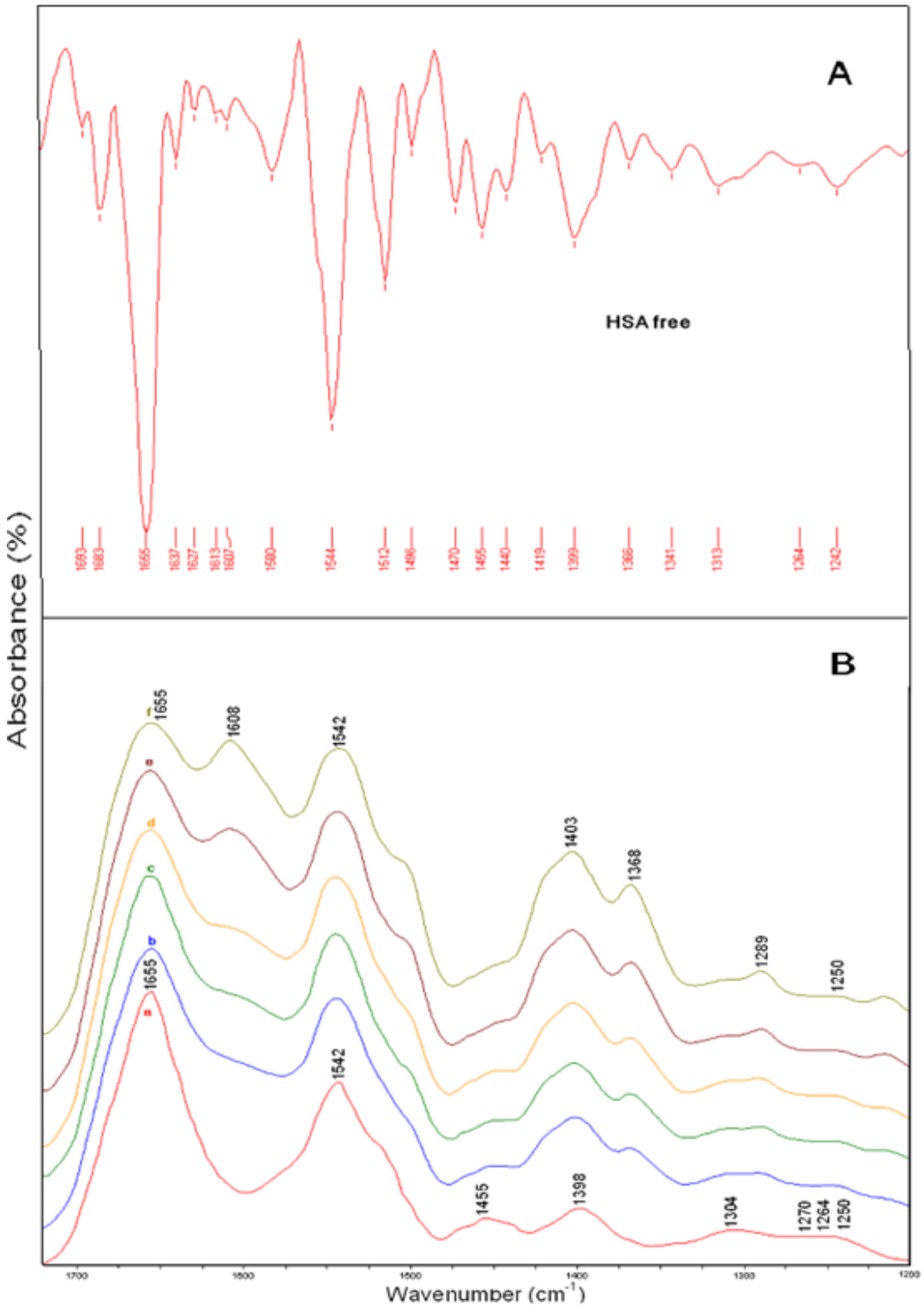

Figure 5. The spectra of (A) HSA free (second derivative) and (a, b, c, d, e, and f) HSA-Ceftriaxone IR absorption spectrum with Ceftriaxone concentrations (0.0, 0.687, 0.910, 1.14, 1.37, and 1.60 mM) respectively.

Determination of the secondary structure of HSA and its ceftriaxone complexes was carried out on the basis of the procedure described by Byler et al. (1986). In this work, a quantitative analysis of the protein secondary structure for the free HSA and ceftriaxone- HSA complexes in dehydrated films is determined from the shape of amides

Table 1. Band assignment in the absorption spectra of HSA with different ceftriaxone concentrations for amide I, II and III regions.

Bands	HSA Free	HSA-Ceft. 0.687mM	HSA-Ceft. 0.910 mM	HSA-Ceft. 1.14 mM	HSA-Ceft. 1.37 mM	HSA-Ceft. 1.60 mM
Amide I (1610-1700 cm^{-1})	1613					
	1626	1627	1625	1629		
	1637	1641	1641	1642	1642	1642
	1655	1654	1655	1656	1657	1658
		1662	1662	1662	1662	1663
	1683	1680	1679	1679	1678	1679
	1693	1693	1693	1692	1692	1692
Amide II (1480-1600 cm^{-1})	1496	1497	1498	1498	1499	1494
	1512	1513	1513	1514	1514	1513
	1544	1545	1546	1536	1535	1536
		1552	1551	1551	1551	1552
		1569	1568	1568	1568	1568
Amide III (1220-1330 cm^{-1})	1580	1586	1585	1585	1586	1584
	1242	1242	1242	1242	1241	1241
	1263	1263	1264	1261	1261	1260
	1303	1288	1288	1288	1288	1288
	1313	1312	1312	1311	1311	1312

I, II and III bands. Infrared Fourier self-deconvolution with second derivative resolution and curve fitting procedures, were applied to increase spectral resolution and therefore to estimate the number, position and area of each component bands. The procedure was in general carried out considering only components detected by second derivatives and the half widths at half height (HWHH) for the component peaks are kept around 5 cm^{-1}; the above procedure was reported in our recent publications (Abu et al., 2011; Darwish et al., 2010; Abu et al., 2012).

The component bands of amides I, II, and III regions were assigned to a secondary structure accor-ding to the frequency of its maximum raised after Fourier self deconvolution have been applied for amide I band ranging from 1610 to 1700 cm^{-1} generally assigned as follows: 1610-1627 cm^{-1} are generally represented to parallel β-sheet, 1627-1643 cm^{-1} represent random coil, 1643-1672 cm^{-1} represent α-helix, 1672-1787 cm^{-1} represent turn structure, and 1687-1700 cm^{-1} represent β-antiparallel. For amide II ranging from 1480 to 1600 cm^{-1}, the absorption band was assigned in the following order: 1485-1502 cm^{-1} represent parallel β-sheet, 1502-1529 cm^{-1} represent random coil, 1529-1563 cm^{-1} represent α-helix, 1563-1587 cm^{-1} represent turn structure, and 1587-1600 cm^{-1} represent β-antiparallel.

For amide III ranging from 1220 to 1330 cm^{-1} was assigned as follows: 1220-1255 cm^{-1} represent parallel β-sheet, 1255-1301 cm^{-1} represent random coil, 1301-1317 cm^{-1} represent turn structure, and 1317-1330 cm^{-1} represent α-helix. Most investigations have concentrated on Amide I band assuming higher sensitivity to the change of protein secondary structure (Vass et al., 1997). However, it has been reported that amide II and amide III bands have high information content and could be used for prediction of proteins secondary structure (Oberg et al., 2004, Jiang et al., 2004, Liu et al., 2003).

Based on the above assignments, the percentages of each secondary structure of HSA were calculated from the integrated areas of the component bands in amide I, amide II and amid III, respectively. Table 2 shows the content of each secondary structure of HSA before and after the interaction with ceftriaxone at different concentrations. The percentage values for the components of amide I of free HSA are consistent with the results of other recent spectroscopic studies.

Figure 6 illustrates the variation of relative intensities with concentration change for the α-helix, parallel and antiparallel β-sheets in HSA free and ceftriaxone-HSA complexes. The results exhibited a reduction of α-helical structures so that of amide II and amide III showed similar trends in their percentage values to that of amide I.

The decrease of α-helix percentage with the increase of ceftriaxone concentrations is evident in the calculations and this trend is consistent in the three Amide regions. However, for the parallel and antiparallel β-sheet, relative percentage increased with increasing ceftriaxone concentrations and the relative intensity increased for the antiparallel β-sheets remarkably having a faster rate increase than the parallel β-sheets.

The reduction of α-helix intensity percentage in favor of

Table 2. Secondary structure determination for amide I, II and III regions for HSA and its ceftriaxone complexes.

Band	HSA Free	HSA-Ceft. 0.687 mM	HSA-Ceft. 0.910 mM	HSA-Ceft. 1.14 mM	HSA-Ceft. 1.37 mM	HSA-Ceft. 1.60 mM
Amide I						
B-sheet parallel (1610-1627 cm^{-1})	10	11	12	13	14	16
Random (1627-1643 cm^{-1})	11	5	4	5	5	7
α-helix (1643-1672 cm^{-1})	68	62	60	45	39	27
Turns (1672-1687 cm^{-1})	8	16	16	24	25	32
B-sheet Anti-parallel (1687-1700 cm^{-1})	3	7	8	13	18	20
Amide II						
B-sheet parallel (1485-1502 cm^{-1})	8	22	24	23	29	33
Random (1502-1529 cm^{-1})	27	9	6	9	4	2
α-helix (1529-1563 cm^{-1})	52	55	55	52	46	43
Turns (1563-1587 cm^{-1})	13	14	13	13	13	14
B-sheet Anti-parallel (1587-1600 cm^{-1})	1	2	3	4	7	9
Amide III						
B-sheet (1220-1255 cm^{-1})	30	20	14	16	14	12
Random (1255-1301 cm^{-1})	19	20	21	20	21	22
Turns (1301-1317 cm^{-1})	29	36	41	41	47	49
α-helix (1317-1330 cm^{-1})	23	25	24	23	19	17

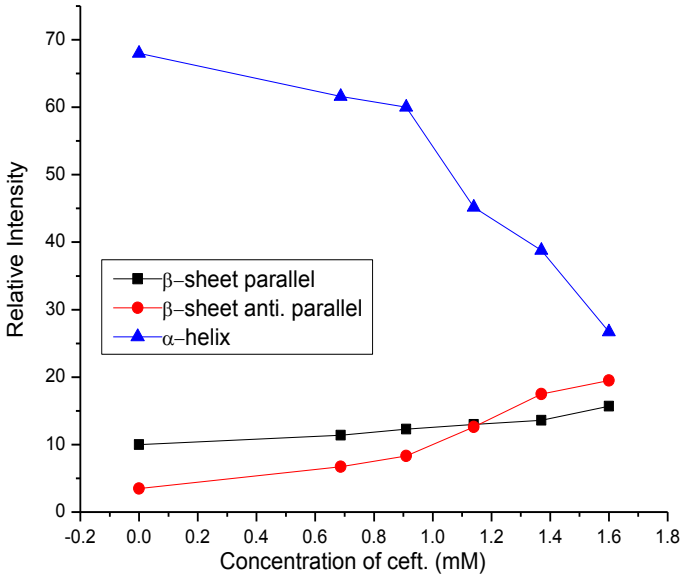

Figure 6. Relative intensities of HSA secondary-structure Amide I components as a function of increasing ceftriaxone concentration. The isolated symbols on the right correspond to the respective secondary structure components.

the increase of β-sheets are believed to be due to the unfolding of the protein in the presence of ceftrixone as a result of the formation of H bonding between HSA and the antibiotic. The newly formed H-bonding result in the C-N bond assuming partial double bond character due to a flow of electrons from the C=O to the C-N bond which decreases the intensity of the original vibrations (Krimm et al., 1986); the hydrogen bonds in α-helix are formed inside the helix and parallel to the helix axis, while for β-sheet, the hydrogen bonds take position in the planes of β-sheets as the preferred orientations especially in the anti-parallel sheets, so the restrictions on the formation of

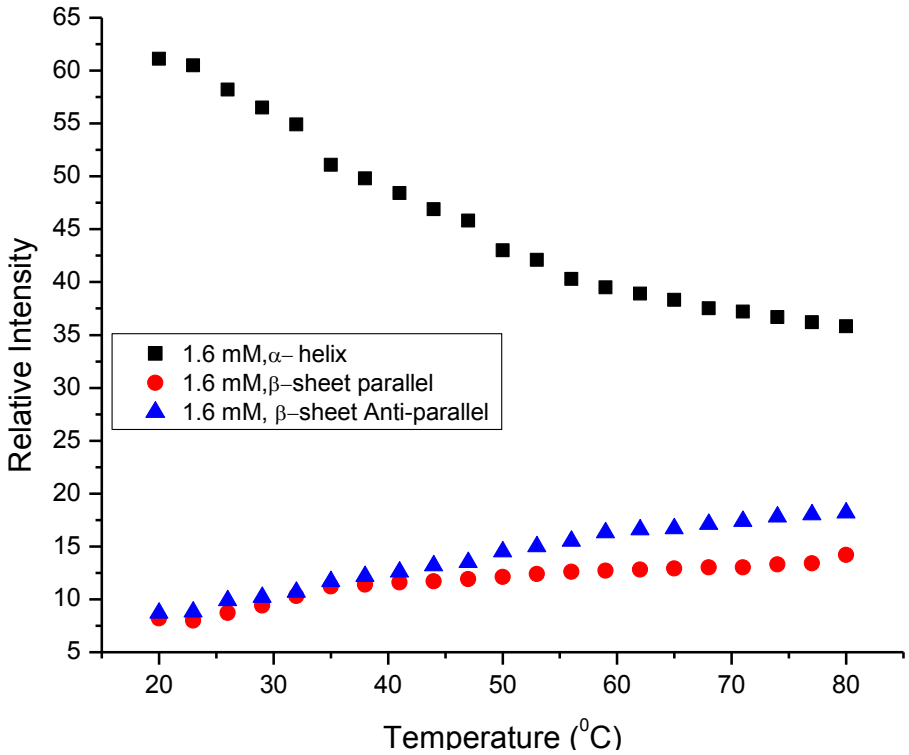

Figure 7. Relative intensities of HSA secondary-structure components at different concentrations ceftriaxone as a function of increasing temperatures. The isolated symbols on the left correspond to the respective secondary structure components.

hydrogen bonds in β-sheet relative to the case in α-helix explains the larger effect on reducing the intensity percentage of α-helix to that of β-sheet. Similar conformational transitions from an α-helix to β-sheet structures were observed for the protein unfolding upon protonation and heat denaturation (Surewicz et al., 1987; Holzbaur et al., 1996).

The variation of intensities with temperature change for α-helix, parallel and antiparallel β-sheets in ceftriaxone-HSA complexes are shown in Figure 7. The relative intensity increases as -temperature and ceftriaxone concentration increases- for the antiparallel β-sheets while it remarkably decreases for α-helix and the rate of increase for antiparallel β-sheets remarkably faster than the parallel β-sheets. The difference in behavior for the two types of β-sheets can be explained by the different amino acids and their preferred secondary structural arrangements in these β-sheets. It has been reported, that the two forms of β-sheets have different thermodynamic propensities scale (Kim et al., 1993).

The slight gradual increase in intensity of the parallel β-sheets is believed to be mainly due to the unfolding of the by fluorescence spectroscopy and by FTIR spectroscopy. From the fluorescence study, we determined values for the binding constant and the quenching constant for ceftriaxone-HSA complexes. The results indicate that the protein as a result of the formation of H-bonding between HSA and ceftriaxone. The newly formed H-bonding result in the C-N bond assuming partial double bond character due to electrons flow from the C=O to the C-N bond which decreases the intensity of the molecular vibrations (Fabian et al., 1993).

On the other hand, an increase of intensity implies more stability and less conversions of the C=O bond as a result of the interaction with ceftriaxone. The parallel arrangement is less stable because the geometry of the individual amino acid molecules forces the hydrogen bonds to occur at an angle, making them longer and thus weaker.

Contrarily, in the anti-parallel arrangement, the hydrogen bonds are aligned directly opposite to each other, making stronger and more stable bonds.

Conclusion

The binding of ceftriaxone to HSA has been investigated

intrinsic fluorescence of HSA was quenched by ceftriaxone through static quenching mechanism. Analysis of the FTIR spectra reveals that HSA-ceftriaxone interaction results in major protein secondary structural changes in

the compositions of α-helix to that of the β-sheets.

The obtained data show an increase in the intensity of the absorption band of the antiparallel βsheets as temperature increases. Higher concentrations of ceftriaxone provide an increase of the absorption band intensity for both the antiparallel and parallel β-sheets.

The intensity analysis is in support of higher stability for the anti-parallel β-sheets compared to that of parallel β-sheets. These variations in behavior are mainly due to the differences in the intrinsic properties of parallel and antiparallel-β sheets. More experimental studies are needed to determine the degree of stability of β-sheets and how does it affect protein folding.

ACKNOWLEDGEMENT

This work was supported by the German Research Foundation DFG Grant No. DR228/24-2.

REFERENCES

Abu Teir MM, Ghithan SJH, Darwish S, Abu-Hadid MM (2011). "Study of Progesterone interaction with Human Serum Albumin: Spectroscopic Approach," J. Appl. Biol. Sci. 5 (13):35-47.

Abu Teir MM, Ghithan SJH, Darwish S, Abu-hadid MM (2012). Multi-spectroscopic investigation of the interactions between cholesterol and human serum albumin. J. Appl. Biol. Sci. 6(3):45-55.

Ahmad B, Parveen S, Khan RH (2006). Effect of albumin conformation on the binding of ciprofloxacin to human serum albumin. Biomacromolecules 7:1350-1356.

Arrondo JL, Muga A (1993). Quantitative studies of the structure of proteins in solution by Fourier-transform infrared spectroscopy. Prog. Biophys. Mol. Biol. 59:23-56.

Artali R, Bombieri G, Calabi L, Del Pra A (2005). A molecular dynamics of human serum albumin binding sites. Il Farmaco 60:485-495.

Bian Q, Xu LC, Wang SL, Xia YK, Tan LF, Chen JF, Song L, Chang HC, Wang XR (2004). Study on the relation between occupational fenvalerate exposure and spermatozoa DNA damage of pesticide factory workers. Occup. Environ. Med. 61:999-1005.

Bibiana N, Beatriz Farruggia, Guillermo Pico (1996). A Comparative study of the binding characteristics of ceftriaxone, cefoperazone and cefsudolin to human serum albumin. Biochem. Mol. Biol. Int. 40(4):823-831.

Bilirubin RB, Alex R (1989). Ceftriaxone binding to human serum albumin. Mol. Pharmacol. 36:478-483.

Brodersen R, Robertson A (1989). Ceftriaxone binding to human serum albumin: competition with biririubin. Mol. Pharnmacol. 36: 478-483.

Byler M and Susi H (1986). Examination of the secondary structure of proteins by deconvolved FTIR spectra. Biopolymers. 25:469-487.

Chen GZ, Huang XZ, Xu JG, Zheng ZZ, Wang ZB (1990). Method of Fluorescence Analysis, Science Press, Beijing,. 112-119.

Cui F, Qin L, Zhang G, Liu X, Yao X, Lei B (2008). A concise approach to 1,11-didechloro-6-methyl-40-O-demethyl rebeccamycin and its binding to human serum albumin: Fluorescence spectroscopy and molecular modeling method. Bioorg. Med. Chem.16:7615-7621.

Cui F, Wang J, Cui Y, Yao X, Qu G, Lu Y (2007). Investigation of interaction between human serum albumin and N6-(2-hydroxyethyl) adenosine by fluorescence spectroscopy and molecular modelling. Luminescence. 22:546-553.

Curry S, Brick P, Franks NP (1999). Fatty acid binding to human serum albumin: new insights from crystallographic studies. Biochem. Biophys. Acta 1441:131-140.

Darwish SM, Abu sharkh SE, Abu Teir MM, Makharza SA, Abu hadid MM (2010). Spectroscopic investigations of pentobarbital interaction with human serum albumin. J. Molecular Structure. 963:122-129.

Fabian H, Schultz C, Naumann D, Landt O, Hahn U, Saenger WJ (1993). Secondary Structure and temperature-induced unfolding and refolding of ribonuclease T1 in aqueous solution: A Fourier transform infrared spectroscopic study. Mol. Biol. 232:967-981.

Ganim Z, Tokmakoff A (2006). Spectral Signatures of Heterogeneous Protein Ensembles Revealed by MD Simulations of 2DIR Spectra. Biophys. J. 91 : 2636.

Guowen Zhang N, Nan Z, Lin W (2011). Probing the binding of vitexin to human serum albumin by multi spectroscopic techniques. J. Lumin 131:880-887.

Hal CP, Thomas PA, Ronald AH, Bliss SP (2000). Simmondsin and wax ester levels in 100 high-yielding jojoba clones. Industrial Crops Prod. 12:151-157.

He XM, Carter DC (1992). Atomic structure and chemistry of human serum albumin. Nature 358:209-215.

Holzbaur IE, English AM, Ismail AA (1996). FTIR study of the thermal denaturation of horseradish and cytochrome c peroxidases in D2O. Biochemistry 35:5488-5494.

Il'ichev AL, Gut LJ, Williams DG, Hossain MS, Jerie PH (2002). Area-wide approach for improved control of oriental fruit moth Grapholita molesta (Busck) (Lepidoptera: Tortricidae) by mating disruption. Gen. Appl. Entomol. 31:7-15.

Jackson M, Mantsch HH (1991). Protein secondary structure from FT IR spectroscopy with dihedral angles from three-dimensional Ramachandran plots. J. Chem. 69:1639-1643.

Jiang M, Xie MX, Zheng D, Liu Y, Li XY, Chen X (2004). Spectroscopic studies on the interaction of cinnamic acid and its hydroxyl derivatives with human serum albumin. J. Mol Structure. 692:71-80.

Kandagal PB, Shaikh SMT, ManjunathaDH, Seetharamappa J, Nagaralli BS (2007). Spectroscopic studies on the binding of bioactive phenothiazine compounds to human serum albumin. J. Photochem. Photobiol. A-Chem. 189(1):121-127.

Kang J, Liu Y, Xie MX, Li S, Jiang M, Wang YD (2004). Interactions of human serum albumin with chlorogenic acid and ferulic acid. Biochimica et Biophysica Acta.1674:205-214.

Kang S, Wu Y, X Li (2004). Effects of statin therapy on theprogression of carotid atherosclerosis: a systematic review and meta-analysis. Atherosclerosis 177(2):433-442.

Kim CA, Berg JM (1993). Thermodynamic beta-sheet propensities measured using a zinc-finger host peptide. Nature 362:267-270.

Kragh-Hansen U (1981). Molecular aspects of ligand binding to serum albumin. Pharmacol. Rev. 33:17- 53.

Krimm S, Bandekar J (1986). Vibrational spectroscopy and conformationof peptides, polypeptides and proteins. Adv. Protein Chem. 38:181-364.

Kumar VK, Ramasamy R (2002). Spectral and normal coordinate analysis of 6-methoxypurine. Indian J. Pure Appl. Phys. 40:252.

Lakowicz JR (1999). Principles of fluorescence spectroscopy. Kluwer Academic Publishers/Plenum Press, Dordrecht/New York.

Lakowicz JR, Weber G (1973). Quenching of protein fluorescence by oxygen. Detection of structural fluctuations in proteins on the nanosecond time scale Biochemistry 12 : 4161.

Li Y, He WY, Dong YM, Sheng F, Hu ZD (2006). Human serum albumin interaction with formononetin studied using fluorescence anisotropy, FT-IR spectroscopy and molecular modeling methods. Bioorg. Med. Chem. 14:1431-1436.

Liu JQ, Tian JN, He WY, Xie JP, Hu ZD, Chen XG (2004). J. Pharm. Biomed. Anal. 35:671.

Liu XP, Du YX, Sun W, Kou JP, Yu BY (2009). Study on the interaction of levocetirizine dihydrochloride with human serum albumin by molecular spectroscopy. Spectrochim. Acta Part A 74:1189.

Liu Y, Xie MX, Kang J, Zheng D (2003). Studies on the interaction of total saponins of panax notoginseng and human serum albumin by Fourier transform infrared spectroscopy. Spectrochim. Acta. Part A. 59:2747-2758.

Locht F, Dorcbe G, Anbert G, Boissier C, Bertrand AM, Branon J (1990). The penetration of ceftriaxone into human brain tissue. J. Antimicrob. Chemother. 26:81-86.

Mcnamara P, TruebV, Stoeckel K (1990). Ceftriaxone binding to human serum albumin. Inderect displacement by probenecid and diazepam. ochem. Pharmacol. 40:1247-1253.

Muravchick S, Smith DS (1995). Parkinsonian symptoms during emergence from general anesthesia. Anesthesiology 82:305-307.
Nerli B, Farruggia B, Picó G (1996). A comparative study of the binding characteristic of of ceftriaxone, cefoperazone and cefsulodin to human
serum albumin. Biochem. Mol. Biol. Int. 40:823-831.
Oberg KA, Ruysschaert JM, Goormaghtigh E (2004). The optimization of protein secondary structure determination with infrared and circular dichroism spectra. Eur. J. Biochem. 271:2937-2948.
Pan J, Ye Z, Cai X, Wang L, Cao Z (2012). Biophysical study on the interaction of ceftriaxone sodium with bovine serum albumin using spectroscopic methods. J. Biochem. Mol. Toxicol. 26:487-492.
Patrick J, Mcnamara VrenyTruebs, Klaus Stoeckel (1990). Ceftriaxone binding to human serum albumin indirect displacement. Biochem. Pharmacol. 40(6):1247-1253.
Peters T (1985). Serum albumin. Adv. Protein Chem. 37:161-245.
Peters T Jr. (1985). Ado. Protein Chem. 37:161-245.
Qing Y, Xi-min Z, Xing-guo C (2011). Combined molecular docking and multi-spectroscopic investigation on the interaction between Eosin B and human serum albumin. J. Lumin. 131:880-887.
Quaglia MG, Bossu E, Dell'Aquila C, Guidotti M (1997). Determination of the binding of a β_2-blocker drug, frusemide and ceftriaxone to serum proteins by capillary zone electrophoresis. J. Pharm. Biomed. Analys. 15:1033-1039.
Rabia S, Shiori T, Leonid B, Sylvie D, Yves F, Dufr E, Vasanthy N, Erik G, Jean-Marie R, Vincent R (2009). Antiparallel β-sheet: a signature structure of the oligomeric amyloid β-peptide Emilie CERF. Biochem. J. 421:415-423.
Reynold Spector (1987). Ceftriaxone transport through the blood-brain barrier. J. Infect. Dis. 156(1):209-211.
Rondeau P, Armenta S, Caillens H, Chesne S, Bourdon E (2007). Assessment of temperature effects on b-aggregation of native and glycated albumin by FTIR spectroscopy and PAGE: Relations between structural changes and antioxidant properties. Archives Biochem. Biophys. 460:141-150.
Royer CA (1995). Approaches to teaching fluorescence spectroscopy. Biophys. J. 68:1191-1195.
Scott VM, William AP Jr, Kristin KJ, Lori K, Joseph AP (2008). Safety of ceftriaxone sodium at extremes of age. Expert Opin. Drug Saf. 7(5):515-523.
Simard AR, Soulet D, Gowing G, Julien JP, Rivest S (2006). Bone marrow-derived microglia play a critical role in restricting senile plaque formation in alzheimer's disease. Neuron 49:489-502.
Sirotkin VA, Zinatullin AN, Solomonov BN, Faizullin DA, Fedotov VD (2001). Calorimetric and Fourier transform infrared spectroscopic study of solid proteins immersed in low water organic solvents. Biochimica et Biophysica Acta. 1547:359-369.
Sudip Bhattacharyya, Tod ES, Jean H, Swank, Craig BMarkwardt (2006). RXTEObservationsof1A1744361: correlated spectral and timing behavior. Astrophys. J. 652:603-609.
Sulkowska A (2002). Interaction of drugs with bovine and human serum albumin. J. Mol. Struct. 614:227-232.
Surewicz WK, Mantsch HH, Chapman D (1993). Determination of protein secondary structure by Fourier transform infrared spectroscopy: A critical assessment. Biochemistry 32:389-394.
Surewicz WK, Moscarello MA, Mantsch HH (1987). Secondary structure of the hydrophobic myelin protein in a lipid environment as determined by Fourier- transform infrared spectrometry. J. Biol. Chem. 262:8598-8609.
Tian JN, Liu JQ, Zhang JY, Hu ZD, Chen XG (2003). Chem. Pharm. Bull. 51:579.
Ulrich H, Cleber AT, Arthur AN 2006). DNA and RNA apta-mers: from tools for basic research towards therapeutic applications. Comb. Chem. High Throughput Screen 9:619-32.
Vandenbussche G, Clercx A, Curstedt T, Johansson J, Jornvall H, Ruysschaert JM (1992). Structure and orientation of the surfactant associated protein C in a lipid bilayer. Eur. J. Biochem. 203:201-209.
Vass E, Holly S, Majer Z, Samu J, Laczko I, Hollosi M (1997). FTIR and CD spectroscopic detection of H-bonded folded polypeptide structures. J. Mol. Struct. 408/409:47-56.
Wang C, Wu Q, Li C, Wang Z, Ma J, Zang X, Qin N (2007). Interaction of tetrandrine with human serum albumin: a Fluorescence quenching study. Analyt. Sci. 23:429-433.
Wang T, Xiang B, Wang Y, Chen C, Dong Y, Fang H, Wang M (2008). Spectroscopic investigation on the binding of bioactive pyridazinone
derivative to human serum albumin and molecular modeling. Colloids Surf. B. 65:113-119.
Workman JR (1998). Applied Spectroscopy: Optical Spectrometers, Academic Press, San Diego. pp. 21-53.
Yue Q, Shen T, Wang C, Gao C, Liu J (2012). Study of the interaction of bovine serum albumin with ceftriaxone and the inhibition effect of Zinc (II). Int. J. Spectrosc. Article ID 284173, doi: 10.1155/2012/284173.
Zhang FL, Jespersen KG, Bjorstrom C, Svensson M, Andersson MR, Sundstrom V, Magnusson K, Moons E, Yartsev A, Inganas O (2006). Influence of guest solvents on the morphology and performance of solar cells based on polyfluorene copolymer/fullerene blends. Adv. Funct. Mater. 16:667-674